

Modulation of the Binding of Signal Peptides to Lipid Bilayers by Dipoles near the Hydrocarbon–Water Interface[†]

L. Voglino,[‡] T. J. McIntosh,^{*,‡} and S. A. Simon[§]

Departments of Cell Biology and Neurobiology, Duke University Medical Center, Durham, North Carolina 27710

Received March 13, 1998; Revised Manuscript Received July 9, 1998

ABSTRACT: Interactions between signal (leader) sequences and membranes are critical to protein insertion and translocation across membranes. In this paper, circular dichroism, tryptophan fluorescence, electrophoretic mobility, dipole potential, and binding measurements were used to study the interaction of the signal sequence of the *Escherichia coli* LamB protein with various lipid bilayers. By modifying specific chemicophysical properties of both the signal sequence and bilayer, we analyzed some of the key factors underlying peptide–lipid interactions. We synthesized three analogues of the LamB signal peptide differing in their net charge (–2 to +4) and studied their binding to bilayers containing combinations of neutral lipids [egg phosphatidylcholine (EPC), sphingomyelin, cholesterol, ketocholesterol, and nitroxide-containing phospholipid] and a charged lipid (phosphatidylserine). All three peptides bound to EPC bilayers and underwent a random coil to α -helix transition upon binding. Microelectrophoresis experiments revealed that both the N and C termini were near the outer surface of the bilayer, suggesting that the peptides adopted a “hammock” configuration with both termini exposed to the aqueous phase and the core of the α -helix located near the hydrocarbon–water interface. The binding of these LamB peptides was not markedly dependent on the bilayer area per molecule, compressibility modulus, or dipole potential, but did depend on the charge of the peptide and bilayer interfacial region. Moreover, the binding of LamB peptides was essentially eliminated in bilayers composed of phospholipids with a nitroxide moiety at the 7 position in one of their acyl chains or in EPC bilayers containing equimolar ketocholestanol. We propose that the incorporation of nitroxide or ketone groups into the hydrocarbon region near the lipid headgroup increases the effective width of the hydrophilic interfacial region and prevents some of the hydrophobic amino acids in the α -helix from reaching the nonpolar hydrocarbon core, thereby diminishing the free energy of partitioning and inhibiting peptide binding. These results point to an important role for interfacial dipoles in peptide–lipid interactions.

The free energy changes associated with the transfer of a peptide or protein from an aqueous phase to a lipid membrane involve several contributions, including electrostatic, hydrophobic, H-bonding, hydration, and van der Waals interactions, and conformational changes in both the peptide and the lipid bilayer (1–9). Studying peptide–bilayer interactions can, in principle, yield fundamental thermodynamic information about the different components of the transfer process, especially when specific chemicophysical aspects of the lipid bilayer and the peptide can be selectively modified. In most previous peptide–bilayer studies, researchers have selectively modified the peptide and chosen a particular type of lipid bilayer (or systematically changed its charge density). For example, the electrostatic component of peptide binding has been nicely demonstrated in a variety of cases by changing the charge density of the lipids and/or increasing the ionic strength (3, 6, 9–12). Attractive electrostatic interactions appear to be the dominant interactions in the case where positively charged peptides bind to bilayers composed of negatively charged lipids. In contrast,

the nonelectrostatic interactions are often more difficult to isolate, although investigators (3, 10) have assumed hydrophobic interactions to be those that are independent of ionic strength. However, even some peptides with large percentages of hydrophobic amino acids, and hence large hydrophobic free energies, do not bind to neutral bilayers (13–15).

Although electrostatic and hydrophobic interactions are of demonstrated importance, other factors, such as the bilayer’s compressibility modulus, area per lipid molecule, dielectric constant, and dipole potential, could, in principle, also influence the binding of peptides to bilayers (7, 16, 17). To address the means by which such interactions may alter peptide binding to bilayers, we have investigated how these factors modulate the binding to lipid bilayers of a well-studied peptide, the signal sequence of the bacterial protein LamB.

In both bacteria and eukaryotes, proteins that are destined to be transported out of the cytoplasm contain N-terminal extension sequences called signal or leader sequences. Prokaryotic and eukaryotic signal sequences share similar features in that both have a net positive charge on their N termini, a hydrophobic portion that adopts an α -helical conformation in hydrophobic environments, and a more polar

[†] This work was supported by Grant GM-27278 from the National Institutes of Health.

[‡] Department of Cell Biology.

[§] Department of Neurobiology.

with different charges near the N and C termini. LamB-EE had negatively charged glutamic acids substituted for the positively charged residues at positions 6 and 7, and LamB-K had the C terminus amidated and also had a lysine at position 25. At neutral pH, LamB-W and LamB-K had three positive charges near their N termini, whereas LamB-EE contained one positive charge and two negative charges near its N terminus (Figure 1).

Preparation of Liposomes. Multilamellar liposomes (MLVs) were made by standard methods (31). Lipids were codissolved in chloroform/methanol (2:1 v:v), and the solvent was removed by rotary evaporation. The lipids were then hydrated in 2 mM Hepes buffer and extensively vortexed.

Small unilamellar vesicles (SUVs) were prepared by probe sonication of MLVs (31). MLVs were sonicated at 40 W with an Excell 2005 sonifier cell disruptor (Heat Systems) with a 19 mm flat tip under continuous N₂ flow for five cycles of 2 min of sonication and 2 min of standing by. Before it was used, the suspension was spun at 100000g for 10 min to sediment metal particles, undispersed lipid, and MLVs. Lipid concentrations were determined by inorganic phosphorus measurements (32).

Large unilamellar vesicles (LUVs) were formed from MLVs using the freeze–thaw high-pressure extrusion method (33). MLVs, at concentrations of 5–15 mg/mL, were frozen and thawed three times and extruded 20 times through a 0.1 μ m polycarbonate filter with a LiposoFast lipid extruder (Avestin, Ottawa, Canada).

X-ray Diffraction. Previous X-ray diffraction studies (34–36) have characterized all of the lipid systems used in this paper except for 7-Doxyl PC. To determine that 7-Doxyl PC formed lipid bilayers, hydrated 7-Doxyl PC was sonicated as described above, frozen and thawed, and pelleted in a bench centrifuge. The pellets were sealed in quartz glass capillary tubes and mounted in a point-collimation X-ray camera. Diffraction patterns were recorded at 20 °C on Kodak DEF X-ray film as described previously (34, 37).

Binding Measurements. The binding of peptides to lipid vesicles was measured with an ultrafiltration assay (38) that separated lipid and lipid–peptide complexes from free peptide with Centrifree (Amicon) filters. In all binding studies, the peptide concentration was 5 μ M, the phospholipid concentration was 1.5 mM, and the buffer was 5 mM Hepes (pH 7.4). This phospholipid concentration was chosen to ensure that the filters did not become clogged. For the binding assay, peptide/SUV or peptide/LUV samples were incubated for 10 min before a 15 min centrifugation at 1000g through the Amicon filter. Control experiments showed that the ratio of the peptide in the filtrate to the peptide in the initial solution was independent of the fraction of volume that was filtered. Peptide recovery in the absence of lipid was greater than 95%, and phosphate analysis (32) revealed that no lipid was in the eluate. The free peptide concentration was measured in the eluate by tryptophan fluorescence at 352 nm. For each peptide/lipid specimen, six ultrafiltrations were performed and six readings taken. The amount of peptide bound to the lipid was determined by subtracting the free peptide concentration from the total peptide concentration. For LamB-W and LamB-EE, experiments were carried out using both LUV and SUVs of EPC and EPC/ketcholestanol. The differences in binding between these two types of bilayers were small (see Results).

The molar partition coefficient K_p was calculated from the binding measurements according to the procedure described by Ladokhin et al. (39). Under our conditions where the molar concentration of peptide in the bilayer is much smaller than the molar concentration of lipid, the mole fraction partition coefficient (K_p) can be written

$$K_p = (P_{\text{bil}}W)/(P_{\text{wat}}L) \quad (1)$$

where P_{bil} and P_{wat} are the bulk molar concentrations of peptide in the bilayer and water phases, respectively, and L and W are the molar concentrations of lipid and water, respectively (39). LamB peptides were presumed to partition only into the outer leaflet of the bilayer (see Discussion). For SUVs, the outer leaflet comprises about 66% of the lipids, and therefore, L was taken to be 66% of the total lipid concentration. The free energies of transfer from buffer to the bilayer were calculated from $\Delta G = -RT \ln K_p$.

Circular Dichroism (CD). CD measurements were taken on an Aviv 62DS spectropolarimeter equipped with a CoolFlow CFT-33 (Neslab) temperature controller. CD spectra of the peptides were obtained at 25 °C using a 1 mm path length quartz cuvette, a 0.5 nm step size, and a 1 s per step acquisition time. Spectra were averaged over 20 scans. For peptides in buffer or SDS, spectra were recorded from 185 to 260 nm. For experiments with neutral bilayers, in which the peptide binding is relatively small (3) and thus has a lower signal-to-noise ratio, peptide–lipid spectra were obtained from 200 to 260 nm and SUVs were used to minimize light scattering. All spectra were baseline-corrected. For peptide–lipid samples, background CD spectra were recorded from buffer with the same lipid concentrations used in the samples. To avoid possible problems with peptide aggregation, 5 μ M peptide was used (27) and lipid concentrations were varied from 0 to 4 mM. Each lipid–peptide sample was prepared independently. Ellipticity measurements at 222 nm, reported as the mean molar residue ellipticity (ϑ_{222}), were measured over an average of 60 points. Standard deviations were less than 10%.

Partition coefficients were also estimated from the CD data by a procedure detailed by White et al. (40). The values of ϑ_{222} as a function of lipid concentration (L) are related to K_p by the relation

$$\vartheta_{222}(L) = [K_p L / (W + K_p L)](\vartheta_{222\text{bound}}) + [1 - K_p L / (W + K_p L)](\vartheta_{222\text{free}}) \quad (2)$$

where $\vartheta_{222\text{bound}}$ and $\vartheta_{222\text{free}}$ refer to the ϑ_{222} values of bound and free peptide, respectively. The value of $\vartheta_{222\text{free}}$ was taken as the measured value of peptide in buffer, and K_p and $\vartheta_{222\text{bound}}$ were used as parameters for fitting to the experimental data (40).

Fluorescence Measurements. Fluorescence emission spectra of the peptide's tryptophan were measured with a Fluoromax DM3000 (Spex Industries, Edison, NJ) photon counting fluorometer operating in the signal/reference mode with a water bath circulator to maintain the temperature at 25 °C. Spectra were collected with a step size of 0.5 nm with an averaging time of 4 s/nm in quartz cuvettes (1.0 or 0.25 cm) over the range of 320–400 nm using an excitation wavelength of 280 nm. SUVs were used to minimize light

scattering. Where appropriate, measurements were corrected for blank suspensions of buffer or lipid in buffer. Blue shifts were calculated as the difference in wavelength of the maxima in the emission spectra of lipid-peptide and peptide samples. For all these experiments, the standard deviation in blue shift was less than 0.5 nm.

Electrophoretic Mobility. The electrophoretic mobility of MLVs was measured at 25 °C using a Rank Brothers Mark 1 unit (Cambridge, England). Measurements of the electrophoretic mobility were obtained at the plane of shear (41), and the apparatus was calibrated using EPC or PS MLVs in 0.1 M NaCl and 5 mM HEPES adjusted to pH 7.0. The EPC vesicles were essentially immobile, whereas the PS vesicles had a mobility of $-4.66 \mu\text{m s}^{-1}/\text{V cm}^{-1}$, consistent with previous measurements (42). For experiments with peptides, each peptide at 20 μM was added to preformed MLVs in a buffer containing 20 mM NaCl, 1 mM Hepes, and 15 mg/mL sucrose (pH 7.4). At least 10 readings were obtained for each experiment.

Dipole Potential. For measurements of the dipole potential (V) of 7-Doxyl PC, monolayers were formed by spreading 20 μL of 20 mg/mL lipid in chloroform on an aqueous subphase in a trough having a surface area of about 20 cm^2 . The subphase was stirred using a small Teflon-coated magnet. Under these conditions, liposomes are in equilibrium with the surface monolayer (43). The dipole potential was measured between a Ag/AgCl electrode in the subphase and an Americium electrode in air connected to a Keithley electrometer. The dipole potential represents the difference in potential in the presence and absence of the monolayer.

RESULTS

Structure of LamB-W, LamB-K, and LamB-EE in Buffer and SDS Micelles

To determine the secondary structure of LamB-W, LamB-K, and LamB-EE (Figure 1) in aqueous and nonpolar environments, CD spectra were obtained for the peptides in buffer and in SDS micelles. In buffer, the three peptides exhibited almost identical spectra (Figure 2A), each with a broad minimum centered at about 200 nm, indicative of random coils (44). A similar spectrum was recorded by McKnight et al. (27) for the wild type LamB signal peptide in buffer. In 10% w:v (346 mM) SDS, the spectra (Figure 2B) of all three peptides were similar and had minima at 208 and 222 nm and a maximum at 195 nm, providing evidence for the presence of α -helices (44). The mean molar ellipticities at 222 nm (θ_{222}) were -12.7 , -11.2 , and $-11.8 \times 10^{-3} \text{ deg cm}^2 \text{ dmol}^{-1}$ for LamB-W, LamB-EE, and LamB-K, respectively. For LamB-W, CD spectra similar to that shown in Figure 2B were obtained in 1 mM SDS (data not shown). McKnight et al. (27) previously found similar spectra for LamB-W in 40 mM SDS and calculated the α -helix content to be 70% in those micelles.

Figure 2C shows the fluorescence emission spectra of LamB-W, LamB-K, and LamB-EE in buffer (dotted lines) and in the presence of 10% SDS (solid lines). In buffer, each peptide had a spectrum with a maximum at 356 nm, which is similar to the value reported by Jones and Gierasch (25) for LamB-W in 5 mM Tris at pH 7.3. In the presence of 10% SDS, the spectrum for each of the three peptides

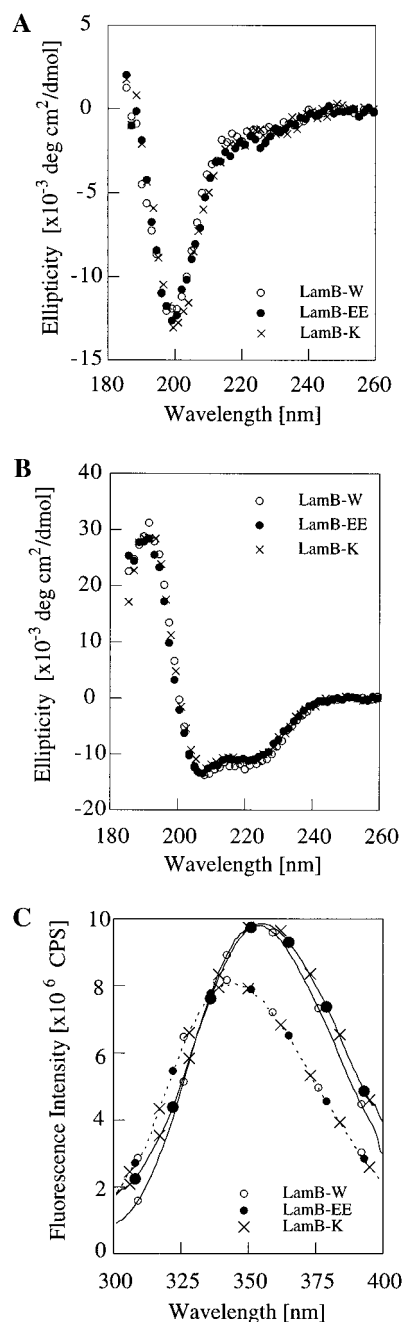


FIGURE 2: Far-UV circular dichroism spectra of 14.3 μM LamB-W, LamB-K, and LamB-EE in (A) 2 mM Hepes buffer (pH 7.4) and (B) 10% (0.346 M) SDS in 2 mM Hepes (pH 7.4) ($R = 2.39 \times 10^4 \text{ SDS/peptide}$). (C) Tryptophan fluorescence spectra of the three peptides in buffer (solid lines) and SDS micelles (dashed lines).

was reduced in intensity and the maximum was displaced to a shorter wavelength of 345 nm, giving a blue shift of 11 nm for all three peptides. This indicates that for each peptide the tryptophan was in an environment with a lower dielectric constant in SDS than in buffer (45).

Interaction of Signal Peptides with EPC Bilayers

Binding experiments showed that there were only small differences in binding between SUVs and LUVs; for LamB-W with 1.5 mM lipid, we obtained a binding of $45.8 \pm 5.6\%$ (mean \pm SEM) to SUVs and $50.9 \pm 3.3\%$ to LUVs. For LamB-EE, we obtained a binding of $33.9 \pm 2.2\%$ to

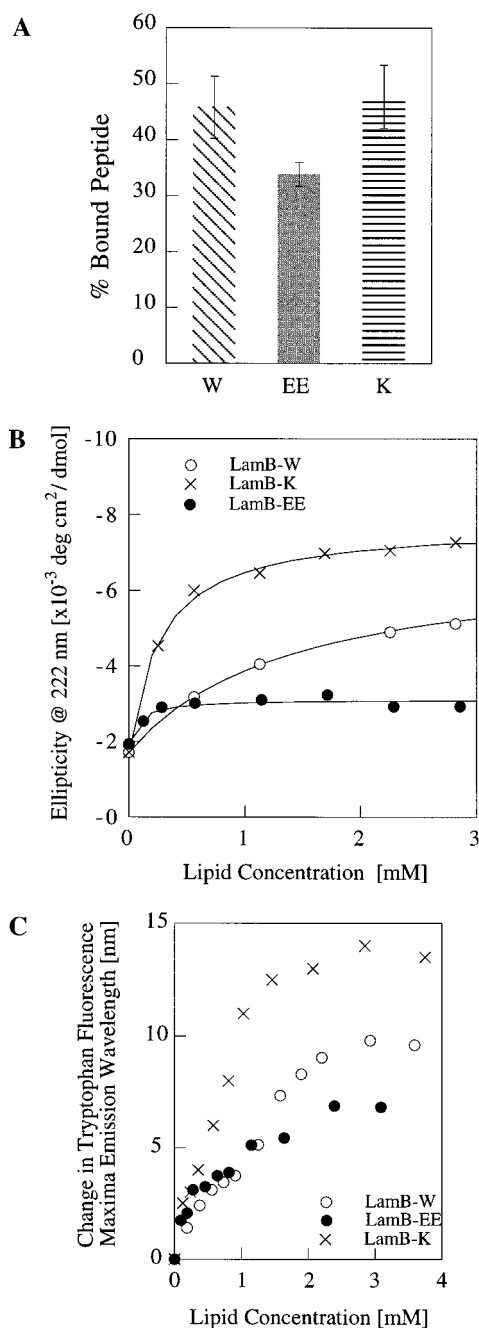


FIGURE 3: Association of LamB-W, LamB-K, and LamB-EE with EPC vesicles at a peptide concentration of 5 μ M in 2 mM Hepes (pH 7.4): (A) percentage of peptide bound to EPC vesicles at a lipid concentration of 1.5 mM, (B) ellipticity at 222 nm (ϑ_{222}), and (C) maximal change in tryptophan fluorescence maxima emission wavelength plotted as a function of EPC concentration. The solid lines in panel B are fits made using eq 2.

SUVs and $34.6 \pm 1.6\%$ ($n = 2$) to LUVs. These results suggest that the binding was not critically dependent on the radius of curvature of the vesicle. Therefore, because CD and blue shift experiments required SUVs, SUVs were used for the binding experiments reported below.

Figure 3A shows the data for binding of the three peptides (5 μ M) to 1.5 mM EPC. The data reveal that the percentage of peptide bound was statistically the same for LamB-W ($45.8 \pm 5.6\%$) and LamB-K ($47.7 \pm 5.6\%$), but significantly lower ($P < 0.001$ using the t test) for LamB-EE ($33.9 \pm 2.2\%$). Thus, for LamB-W, there were 2.29μ mol bound

Table 1: Parameters for Peptide Binding to SUVs in 5 mM Hepes at pH 7.4

| peptide | lipid | % bound peptide (mean \pm SEM) | K_p | $-\Delta G$ (kcal/mol) |
|---------|--------------|-------------------------------------|--------------------|---------------------------|
| LamB-W | EPC | 45.8 ± 5.6 | 4.65×10^4 | 6.3 |
| LamB-K | EPC | 47.7 ± 5.6 | 5.02×10^4 | 6.3 |
| LamB-EE | EPC | 33.9 ± 2.2 | 2.82×10^4 | 6.0 |
| LamB-W | 4:1 EPC/PS | 94.4 ± 0.9 | 9.27×10^5 | 8.0 |
| LamB-EE | 4:1 EPC/PS | 34.8 ± 2.3 | 2.94×10^4 | 6.0 |
| LamB-W | DAPC | 42.4 ± 4.8 | 4.06×10^4 | 6.2 |
| LamB-W | 1:1 EPC/chol | 43.9 ± 3.1 | 4.30×10^4 | 6.2 |
| LamB-W | 1:1 EPC/keto | 3.7 ± 1.8 | 7.58×10^2 | 3.9 |
| LamB-W | 7-Doxyl PC | 0.8 ± 1.0 | 1.61×10^2 | 3.0 |
| LamB-W | 1:1 SM/chol | 47.0 ± 5.9 | 4.89×10^4 | 6.3 |

for 1.5 mM EPC. If the peptide were confined to the outer monolayer of the bilayer, then there was one LamB-W molecule per approximately 327 lipid molecules.

From these binding data, the molar partition coefficients, K_p , were calculated from eq 1 and are given in Table 1. From these partition coefficient experiments, the molar free energy of transfer of the peptide from the aqueous phase to the EPC bilayer (ΔG) was obtained using $\Delta G = -RT \ln K_p$. For EPC, the molar free energies of all three peptides were between -6.0 and -6.3 kcal/mol (Table 1).

Figure 3B shows that the ellipticity at 222 nm (ϑ_{222}) of each peptide increased in a sigmoidal manner with increasing EPC concentrations. Therefore, the amount of α -helix increased with increasing lipid concentration. The complete CD spectra obtained with increasing lipid concentrations (not shown) displayed an isodichroic point at 205 nm, indicating that in buffer with various concentrations of EPC there were primarily two populations of these peptides (46), random coils and α -helices. For the maximal CD response ($\vartheta_{222\text{max}}$) we found that LamB-K > LamB-W > LamB-EE. Thus, the more positive the charge on the peptide, the greater the change in CD and the percentage of α -helix. The percentage of helix for LamB-K, LamB-W, and LamB-EE in EPC bilayers compared with the percentage of helix found in SDS micelles was 59, 38, and 28%, respectively. In this regard, McKnight et al. (27) also found the molar ellipticity to be lower in PE/PG (65:35) vesicles than in SDS micelles, although their observed differences were smaller.

The solid lines in Figure 3B represent fits to the CD data made using eq 2 with K_p and $\vartheta_{222\text{bound}}$ as fitting parameters (40). The values obtained for K_p were 5.8×10^4 , 3.05×10^5 , and 9.3×10^5 for LamB-W, LamB-K, and LamB-EE, respectively. For LamB-W, where most CD experiments were performed, there was quite reasonable agreement with the value of 4.7×10^4 obtained from the direct binding experiments (Table 1). However, the values obtained for LamB-K and LamB-EE were larger than the values obtained from binding experiments (Table 1). In particular, due to the low amount of binding and the resulting noisy CD data, the K_p values obtained from CD for LamB-EE were not as reliable as those obtained from the binding experiments. For this reason, and because the binding experiments are more direct, for the remaining lipids we relied on binding experiments to determine K_p and ΔG .

Figure 3C shows the change in the wavelength of the maximum of tryptophan fluorescence (blue shift) versus lipid concentration for the three peptides. For all three peptides, the blue shifts increased monotonically with increasing lipid

Table 2: Electrophoretic Mobility Measurements of LamB Peptides with Lipids^a

| lipid | peptide | electrophoretic mobility ($\mu\text{m s}^{-1}/\text{V cm}^{-1}$) |
|--------------|--------------|---|
| EPC | none | -1.01 ± 0.083 |
| 1:1 EPC/keto | none | -1.01 ± 0.091 |
| EPC | LamB-W (+2) | -0.59 ± 0.11 |
| EPC | LamB-K (+4) | 0.97 ± 0.22 |
| EPC | LamB-EE (-2) | -1.27 ± 0.13 |

^a Experiments with peptides were performed with a concentration of 20 μM peptide in the presence of 20 mM NaCl, 1 mM Hepes, and 15 mg/mL sucrose at pH 7.4.

concentration in a manner similar, but not identical, to the differences in ellipticity (Figure 3B). In particular, the order LamB-K > LamB-W > LamB-EE was the same order found for $\vartheta_{222\text{max}}$ (Figure 3A). Very similar blue shift data were obtained for LamB-W and EPC bilayers in 2 mM Hepes buffer in the absence of salt (Figure 3C) and with 150 mM NaCl (data not shown), indicating that electrostatic interactions did not make a major contribution to the interaction between LamB-W and EPC.

Microelectrophoresis Experiments

Since all three peptides bound to EPC bilayers (Figure 3A), we performed microelectrophoresis experiments to obtain information regarding the position of their N and C termini. Table 2 shows the mobility of EPC MLVs in the absence and presence of peptide in 20 mM NaCl at pH 7. For EPC liposomes, μ was negative, meaning that the EPC liposomes were negatively charged. This behavior has been found by numerous researchers and probably arises from trace amounts of fatty acid (47). For EPC, we determined using the Gouy–Chapman equation (48) that there was one negative charge for every 59 lipid molecules. The addition of peptides increased or decreased this charge density. We also found that, as expected from its structure (Figure 1), the incorporation of equimolar ketocholestanol into EPC did not alter the electrophoretic mobility (Table 2).

In the presence of 20 μM LamB-W (+2 net charge in buffer), μ decreased (toward 0 mV), and in the presence of 20 μM LamB-K (+4), μ changed sign to become positive. In contrast, μ became more negative in the presence of the negatively charged LamB-K (-2). As described in the Discussion, these data indicate that both the N and C termini were on the same side of the bilayer.

Role of Lipid in Modulating the Binding of Signal Peptides

Surface Charge. Numerous studies have shown that positively charged peptides bind more strongly to negatively charged lipids than to neutral lipids (9, 10, 12). To determine whether this was also true for the LamB peptides, we compared the binding, molar ellipticity (ϑ), and blue shift of LamB-W (+2 net charge), as well as those of LamB-EE (-2), to those of neutral (EPC) and negatively charged (4:1 EPC/PS) vesicles. Panels A–C of Figure 4 show that for LamB-W, the presence of PS produced a marked increase in binding, $\vartheta_{222\text{max}}$, and blue shift, whereas for LamB-EE the presence of PS had small effects on these parameters. The inclusion of PS in EPC vesicles increased the amount

of binding of LamB-W from 45.8 to 94.4% (Table 1), the latter value corresponding to one LamB-W molecule for every 158 lipids. The presence of PS produced a 20-fold increase in the LamB-W molar partition coefficient (K_p), corresponding to a 1.70 kcal/mol increase in the free energy of transfer (Table 1).

Compressibility Modulus. Two factors that should be considered in peptide–bilayer interactions are the work to separate the acyl chains when a peptide penetrates into a lipid bilayer and the bending, or curvature-elastic energy, that results from an energy imbalance between the two monolayers as a result of asymmetric peptide binding. A parameter that characterizes both these work terms is the isothermal compressibility modulus, K_T (49, 50). For liquid-crystalline bilayers, this modulus ranges from about 100 dyn/cm for DAPC bilayers to about 1800 dyn/cm for equimolar sphingomyelin (SM)/cholesterol bilayers (35, 36). To determine the role of the compressibility modulus on signal peptide interaction, we measured the amount of binding of LamB-W to zwitterionic bilayers comprised of DAPC ($K_T = 100$ dyn/cm), EPC ($K_T = 192$ dyn/cm), equimolar EPC/cholesterol ($K_T = 660$ dyn/cm), equimolar EPC/ketocholestanol ($K_T = 370$ dyn/cm), and equimolar SM/cholesterol ($K_T = 1800$ dyn/cm). Figure 5A and Table 1 show that the amount of binding of LamB-W was similar for bilayers composed of EPC, EPC/cholesterol, DAPC, and SM/cholesterol but was significantly smaller for bilayers of EPC: ketocholestanol. In particular, LamB-W bound to EPC bilayers to approximately the same extent in the presence and absence of cholesterol ($\approx 45\%$), whereas only about 4% of LamB-W was bound to 1:1 EPC/ketocholestanol bilayers ($3.7 \pm 1.8\%$ bound to SUVs and $1.5 \pm 1.8\%$ bound to LUVs). This amount of binding to EPC/ketocholestanol SUVs is statistically significantly different than zero binding ($P < 0.001$), but nevertheless reflects a 20-fold decrease in K_p compared to that of EPC (Table 1). The incorporation of equimolar ketocholestanol into EPC bilayers caused a decrease in free energy of about 2 kcal/mol (Table 1). Thus, the effect of ketocholestanol was very different from that of cholesterol in that ketocholestanol, unlike cholesterol, markedly reduced the amount of binding of LamB-W to EPC bilayers (Figure 5A and Table 1).

That the amount of LamB-W binding was about the same to EPC and DAPC bilayers implies that binding was insensitive to the molecular area, at least between 64 (EPC) and 76 \AA^2 (DAPC) (51). This observation is consistent with our result that LamB-W and LamB-EE bound to SUVs and LUVs in similar amounts, which, because of curvature constraints, have different areas per molecule in the outer monolayer of the bilayer (52).

To further document the effect of cholesterol and ketocholestanol on peptide–lipid interactions, we performed CD and blue shift measurements. Both ellipticity (Figure 5B) and blue shift (Figure 5C) changes were in the order EPC > EPC/cholesterol \gg EPC/ketocholestanol ≈ 0 . Similar blue shift data were recorded for LamB-EE with EPC, 1:1 EPC/cholesterol, and 1:1 EPC/ketocholestanol (data not shown).

Figure 6A shows the free energies of transfer of LamB-W plotted versus the isothermal compressibility moduli (K_T). There does not appear to be a correlation between binding and bilayer compressibility. The major point is that the

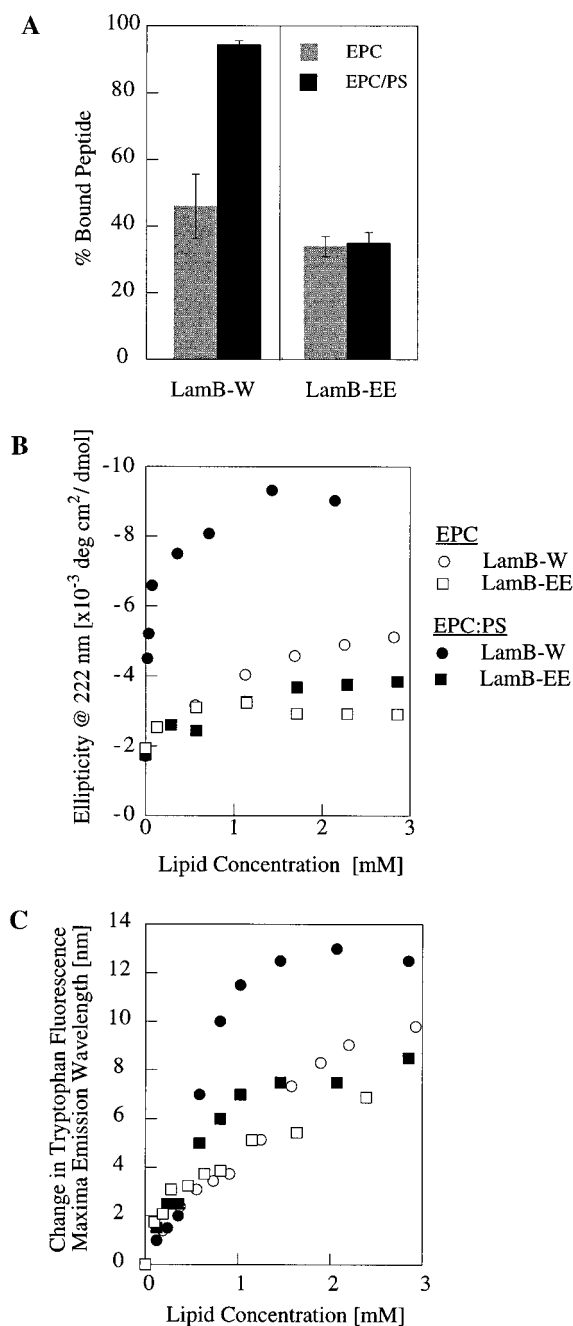


FIGURE 4: Effects of surface charge on the association of LamB-W and LamB-EE with lipid bilayers at a peptide concentration of 5 μ M: (A) percentage of LamB-W and LamB-EE bound to EPC and 4:1 EPC/PS vesicles at a lipid concentration of 1.5 mM, (B) ϑ_{222} , and (C) blue shift plotted as a function of lipid concentration for both EPC and 4:1 EPC/PS vesicles. The same symbols are used in panels B and C.

binding was significantly smaller for EPC/ketocholesterol than for any of the other lipids, and this difference was not related to K_T .

Dipole Potential and Interfacial Dipoles. The observations (Figure 5A–C) that the interaction of LamB-W differs among EPC, EPC/cholesterol, and EPC/ketocholesterol bilayers indicates that small differences in the interfacial region of the bilayer can have large effects on the interaction of peptides with bilayers. The major structural difference between cholesterol and ketocholesterol is the presence of a ketone group at position 6 of ketocholesterol (Figure 1). Thus, ketocholesterol has dipolar hydroxyl (OH) and ketone

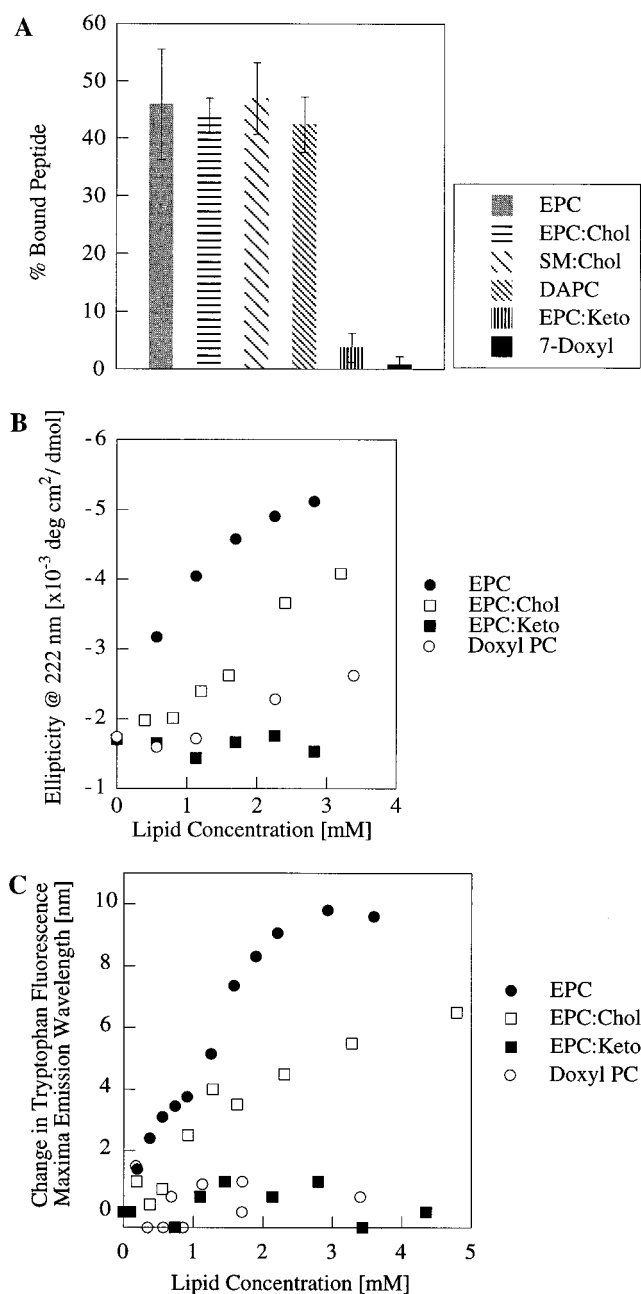


FIGURE 5: Association of LamB-W with EPC, DAPC, 1:1 EPC/cholesterol, 1:1 EPC/ketocholesterol, and 7-Doxyl PC at a peptide concentration of 5 μ M: (A) percentage of LamB-W bound to bilayers at a lipid concentration of 1.5 mM, (B) ϑ_{222} , and (C) blue shift vs lipid concentration.

(O=C) groups that are separated by about 4 Å. X-ray diffraction (36), permeability, and binding measurements (53) indicate that ketocholesterol is oriented nearly perpendicular to the plane of the bilayer, meaning that the ketone group is located about 4 Å deeper in the bilayer's hydrocarbon region than the OH group, which is anchored near the hydrocarbon–water interface at the level of the deeper carbonyl group (54, 55).

One possibility for rationalizing the dramatic effect of ketocholesterol incorporation on the binding of LamB-W to EPC bilayers is that ketocholesterol increases the dipole potential (i.e., makes the interior of the membrane more positive), and it has been suggested that peptide binding might be affected by bilayer dipole potential (56). The dipole

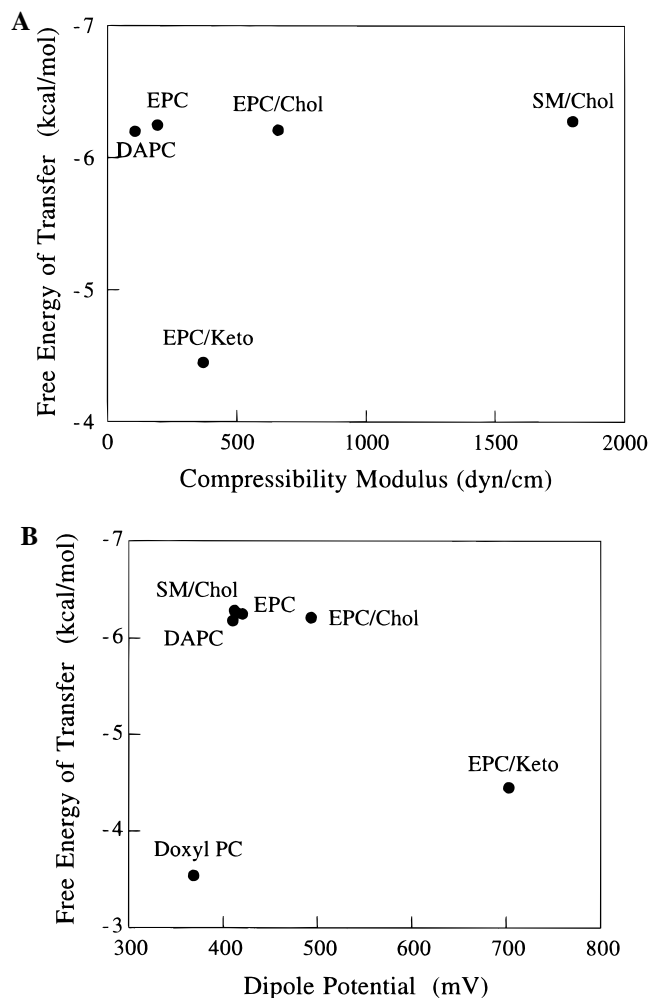


FIGURE 6: Correlation between free energy of transfer of LamB-W and (A) bilayer isothermal compressibility moduli (K_T) and (B) dipole potential (V). Values of K_T were taken from refs 51, 72, and 73, and values of V were taken from refs 73 and 74 and from this study (7-Doxyl PC).

potential of EPC is 415 mV, and the dipole potential of equimolar EPC/ketocholestanol is 703 mV as measured for lipid monolayers (36). Because ketocholestanol has a large dipole (the ketone moiety) located in the hydrocarbon region of the bilayer, we tested whether other lipids with dipoles located at similar depths in the hydrocarbon region would also decrease peptide binding, or whether this effect was specific to ketocholestanol. Another lipid with a large dipole located in its hydrocarbon region is 7-Doxyl PC, which has a nitroxide moiety at position 7 on one of its acyl chains (Figure 1). In liquid-crystalline bilayers, the distance between CH_2 groups along an acyl chain is about 0.9 \AA per CH_2 group (57). Therefore, in bilayers of 7-Doxyl PC, the nitroxide should be located about 5 \AA from the carbonyl group (Figure 1), or, on average, about the same depth from the hydrocarbon–water interface as the ketone group is in EPC/ketocholestanol bilayers. X-ray diffraction showed that pure 7-Doxyl PC forms liquid-crystalline bilayers; X-ray patterns from fully hydrated 7-Doxyl PC contained two orders of a lamellar repeat period of 65 \AA and a broad wide-angle band at 4.5 \AA (data not shown). Such patterns are characteristic of liquid-crystalline phase bilayers (58).

Figure 5A and Table 1 show that the amount of binding of $5 \mu\text{M}$ LamB-W to 1.5 mM lipid was in the order $\text{EPC} \approx$

$\text{EPC/cholesterol} \gg \text{EPC/ketocholestanol} \approx 7\text{-Doxyl PC}$. Panels B and C of Figure 5 show that at all lipid concentrations both the ellipticity changes and blue shift for LamB-W associating with 7-Doxyl PC bilayers were similar to those for EPC/ketocholestanol bilayers, and much lower than those for EPC bilayers. Thus, all three techniques (Figure 5A–C) indicate the binding of LamB-W to 1:1 EPC/ketocholestanol and 7-Doxyl PC bilayers was similar.

To determine if the observed similarity in binding properties of EPC/ketocholestanol and 7-Doxyl PC bilayers was correlated with dipole potential (V), we measured V for 7-Doxyl PC monolayers. We found V equals $368.7 \pm 9.2 \text{ mV}$ for 7-Doxyl PC, significantly lower than the V value of 703 mV for equimolar EPC/ketocholestanol (36). Thus, even though both 7-Doxyl PC and EPC/ketocholestanol have large dipoles located at similar positions in the hydrocarbon region of the bilayer, they have quite different dipole potentials as measured with monolayers. This implies that the orientation of the ketone and nitroxide dipoles must be different. Figure 6B shows that there is no correlation between the measured free energies of transfer of LamB-W (from Table 1) and the measured dipole potentials for EPC, DAPC, 1:1 EPC/cholesterol, 1:1 EPC/ketocholestanol, 1:1 SM/cholesterol, and 7-Doxyl PC.

DISCUSSION

Our binding, CD, fluorescence, and microelectrophoresis experiments provide information both on the conformation of the LamB signal peptide in bilayers and on the effects that changes in the bilayer interfacial (headgroup) region have on the association of helices with bilayers.

Conformation of LamB Signal Peptides in SDS Micelles and EPC Bilayers. CD and tryptophan fluorescence measurements (Figure 2) revealed that LamB-W, LamB-EE, and LamB-K each had a random coil conformation in buffer and an α -helical conformation in SDS micelles, with the tryptophan residue in a low-dielectric environment. The values of ϑ_{222} and fluorescence emission wavelength were similar for all three peptides in SDS, implying that these three peptides with different net charges (Figure 1) had similar conformations when they were associated with the highly negatively charged SDS micelles. Thus, nonelectrostatic (hydrophobic) interactions must be critical in the association of these peptides with SDS.

In contrast to the similar CD and tryptophan fluorescence data found for all three peptides in SDS, in EPC vesicles the maximum values obtained from these two measurements were markedly different for the different peptides (panels B and C of Figure 3). This implies that, unlike SDS, the polar headgroup region of EPC bilayers can distinguish among the three peptides and influence their binding and/or conformation. That the three peptides had the same average conformation in buffer (Figure 2A) means that any differences in the amount of peptide binding to bilayers reflects changes in their interaction with the bilayer. One factor that could explain the higher ellipticity in EPC seen with LamB-K compared to that with LamB-W is the fact that the positive charge near the C terminus may stabilize the helix in the bilayer, as charged groups near the end of small peptides can stabilize helix formation (59). In contrast, the differences in ellipticity and blue shift between LamB-W

and LamB-EE can be, at least in part, explained by a smaller amount of binding of LamB-EE to the bilayer (Figure 3A).

Factors that could contribute to the observed differences in the interactions of the three peptides with SDS micelles and EPC bilayers include electrostatics, since EPC is electrically neutral and SDS is negatively charged. However, electrostatics alone cannot explain why the negatively charged LamB-EE has a larger change in ellipticity in the presence of SDS micelles than in the presence of EPC bilayers. Another factor, described in detail below, is the wider and more complex interfacial region of EPC compared to the region of SDS.

Location of LamB N and C Termini. For LamB-W, there is agreement that the N terminus is confined to the outer monolayer, especially for bilayers containing negatively charged lipids (25, 28, 29). However, one study (29) found that the C terminus was also located on the outside of the vesicle, whereas others (25, 28) have presented models with the C terminus penetrating to various extents into the bilayer acyl chain. Jones and Gierasch (25) argue against a model with both termini on the same side of the bilayer because of the unfavorable energy associated with breaking backbone H bonds in creating a reverse turn in the hydrophobic region. However, given the fact that the energy needed to break H bonds between NH and O=C in nonpolar environments is about 6 kcal/mol (60), whereas the Born plus image energy required to transfer a univalent charge in the hydrocarbon region is at least 40 kcal/mol (61), it is not evident which of the terms would be larger, especially since the entire α -helix may not be completely buried in the hydrocarbon region and some of the H bonds that are broken could be made up by H bond donating and accepting moieties in the interfacial region.

The electrophoretic mobility experiments (Table 2) provide evidence that both the N and C termini of LamB-W were on the outside of EPC vesicles. Electrophoretic mobility measurements with MLVs are sensitive to charges near the plane of shear which is located outside of the vesicle near the polar headgroup (41, 42). Peptide charges in the fluid space inside the vesicle would not contribute appreciably to the electrophoretic mobility because of they are located more than 50 Å from the plane of shear and the screening of counterions. At low ionic strengths, the addition of the same concentration of each of the three peptides changed the mobility of EPC in a manner expected from their net charge, assuming that the C and N termini were fully charged at pH 7. LamB-W (+2 net charge) or LamB-K (+4) increased the mobility in a more positive direction with the amount of increase greater for LamB-K, whereas LamB-EE (−2) changed the mobility in a more negative direction (Table 2). This suggests that all of the charges were on the outside of the bilayer.

Comparisons of the mobilities of vesicles with that of each of the three peptides provide additional evidence that both termini were on the outside of the vesicle. First, consider LamB-W and LamB-EE, which are chemically identical except that the two positive amino acids near the N terminus in LamB-W were changed to negatively charged residues in LamB-EE (Figure 1). The fact that LamB-EE increased the mobility of EPC vesicles in a negative direction whereas LamB-W decreased the mobility means that the negative charges (E and E) and positive charges (R and K) near the

N termini of these peptides must be on the outside of the vesicle. The implicit assumption is that the localization of the termini and their contribution to the mobility were unaffected by these two amino acid substitutions, and indeed, the molar ellipticities and blue shifts of these two peptides with EPC were similar (Figure 3B,C). In addition, compared to EPC vesicles, LamB-W and LamB-EE caused similar changes in electrophoretic mobility, although in opposite directions. This provides evidence that the total charge on the outside of the bilayer was of the same magnitude, but had opposite signs, for the vesicles containing LamB-W and LamB-EE. This result is consistent with these peptides having all their charged groups on the outside of the vesicle (+2 net charge for LamB-W and −2 net charge for LamB-EE), but inconsistent with the peptides having a transbilayer organization (+3 net charge on the outside of the vesicle for LamB-W and −1 net charge for LamB-EE). This shows that the N terminus of LamB-W did not require negatively charged lipids to anchor it to the aqueous phase.

LamB-K, which is the same sequence as LamB-W except for the amidation of the C terminus and the addition of a positive charge at the amino acid next to the C terminus (Figure 1), imparted a more positive charge to EPC than LamB-W (Table 2). This suggests that both of LamB-K's termini were on the same side of the membrane. Because LamB-W and LamB-K had the same concentration in the bilayer (Figure 3A) and the mobility was greater for LamB-K than LamB-W, it is likely that for LamB-K all four positive charges contributed to the mobility and were therefore on the same side of the bilayer. If it were postulated that the charged C termini in LamB-W and LamB-K crossed the membrane, then both LamB-W and LamB-K would have three positive charges on the outer surface and should have approximately the same mobility. The fact that they did not (Table 2) indicates that the positive charge near the C terminus of LamB-K was on the same side as the N terminus. Thus, for all three peptides, we conclude that both the N and C termini were on the same side of the bilayer.

Taken together, the observations that (1) LamB-W formed an α -helix in EPC bilayers, (2) both its N and C termini were on the same side of the bilayer, and (3) its tryptophan in position 18 penetrated about 9 Å into the hydrocarbon region (25) suggest that LamB-W adopts a “hammock” configuration in the bilayer, with both termini exposed to the aqueous phase, and its α -helix near the interfacial region. Such a hammock configuration would not necessarily involve a reverse turn in the helix region, especially if the α -helix were oriented nearly parallel to the bilayer surface. Moreover, the “helix breaker” glycine located in position 17 (in the middle of the string of nonpolar and uncharged residues of LamB-W) could provide flexibility near the middle of the helix.

Partitioning of LamB Peptides into Bilayers. The partitioning of a peptide into a bilayer involves the adsorption of the peptide to the interface, subsequent conformational changes in the peptide and membrane, and an insertion step (62, 63). The free energy of transfer (ΔG) is the algebraic sum of several positive and negative terms (3, 7, 12, 63, 64). Although many of these terms can be quite large, in the case of LamB-W binding to EPC the free energy of binding was determined to be the relatively small value of −6.3 kcal/mol (Table 1). To place this number in perspec-

tive, it is about equal to the energy needed to transfer three nonpolar amino acid residues from water into a PC bilayer (60).

A major factor promoting adsorption and insertion of LamB-W into neutral bilayers is the hydrophobic free energy (3). For LamB-W, the maximal hydrophobic contribution (assuming all hydrophobic amino acids were completely buried in the hydrocarbon region) was calculated to be -55 kcal/mol (3). However, in analyzing the LamB-W binding to PG/PE bilayers, Jones and Gierasch (3) concluded that only about 30% of the maximum hydrophobic effect was realized, "presumably because of losses from polar head-group effects". Our observation that the binding of LamB-W to EPC was not modified by an increase in ionic strength is consistent with the idea that nonelectrostatic interactions such as hydrophobic interactions play a major role in the binding to these neutral bilayers.

Electrostatics play an important role in the binding of LamB-W to negatively charged bilayers, as has been shown for many positively charged peptides and proteins (9, 11, 65–67). For LamB-W binding to 65:35 PE/PG bilayers, Jones and Gierasch (3) demonstrated the importance of electrostatics by showing that as the ionic strength was increased the transfer free energy changed from -11.4 to -5.1 kcal/mol. This high-ionic strength value is similar to our measured value (Table 1) of ΔG of -6.3 kcal/mol for LamB-W binding to electrically neutral EPC bilayers.

The addition of 20% PS to EPC did not significantly alter the amount of LamB-EE binding (Figure 4A), even though, if electrostatics were the only factor involved, it might be expected that PS would decrease the amount of binding of LamB-EE (-2 net charge in buffer) about as much as it increased the amount of binding of LamB-W ($+2$). There are at least two possible explanations. (1) Because the presence of PS lowers the pH near the bilayer surface (68), the glutamic acids of LamB-EE might be closer to their pK_a 's and therefore not fully charged. (2) Electrostatic effects can be neutralized by other interactions, such as hydrophobic interactions.

Effects of Ketocholestanol on Peptide Binding. The addition of equimolar ketocholestanol to EPC has a dramatic effect on LamB-W binding, markedly reducing the amount of binding to EPC from 46 to 4% (Figure 5A) and the molar partition coefficient by a factor of 60 (Table 1). These binding data are completely consistent with the CD spectra which show that for EPC/ketocholestanol bilayers there is little α -helix formation (Figure 5B) and the tryptophan fluorescence measurements which showed that in the presence of EPC/ketocholestanol bilayers the tryptophan at position 18 was not in a low-dielectric environment (Figure 5C). The generality of these observations with respect to other types of peptides is not known at present. Cladera and O'Shea (69) used fluorescent probe measurements to determine the interaction of the mitochondrial amphipathic signal sequence p25 with EPC in the presence and absence of ketocholestanol. They found that 15 mol % ketocholestanol had little effect on the dissociation constant, but increased the p25 binding "capacity", and modified the conformation of the peptide. Thus, even small concentrations of ketocholestanol can affect the interaction of peptides with bilayers.

A central issue is determining the mechanisms by which ketocholestanol destabilizes the interaction between LamB-W and the bilayer. Several possible factors can be eliminated. First, because EPC/ketocholestanol bilayers have the same electrophoretic mobility and hence surface charge density as EPC bilayers (Table 2), the difference in binding properties of these bilayers cannot be due to electrostatic interactions. Second, effects of changes in bilayer structure (e.g., area per molecule) can be eliminated because the incorporation of ketocholestanol into EPC bilayers has little effect on bilayer organization (36) and there is a lack of correlation between binding and the bilayer compressibility modulus (Figure 6A). A third possibility that can be eliminated is the increase in dipole potential (V) caused by the incorporation of ketocholestanol into EPC (36). For phospholipids such as EPC, the large positive V has been shown to increase the amount of binding of hydrophobic anions and decrease the amount of binding of hydrophobic cations that partition into the interfacial region of the bilayer (56, 70). Since proteins and peptides have fixed charges and large dipole moments (71), it has been proposed that V can influence their adsorption to bilayers (56). However, if the dipole potential were an important factor in the interactions between LamB peptides and bilayers, one would expect that LamB-EE (-2) would bind more avidly than LamB-K ($+4$) or LamB-W ($+2$) to both EPC and EPC/ketocholestanol bilayers which have positive dipole potentials. The fact that it did not (Figure 3A) provides evidence that the dipole potential is not a major factor in the binding of these peptides to these bilayers. Moreover, the data in Figure 6B show that there is no correlation between the amount of LamB-W binding and dipole potential.

Ketocholestanol's Effects on Interfacial Width. Another factor to consider in LamB-W partitioning into the bilayer is the location of the polar ketone group in EPC/ketocholestanol bilayers. As noted in the Results, the ketone group is located about 4 \AA into the bilayer's hydrocarbon region (see Figure 1) and energetic calculations suggest that the ketone group is hydrated (36). Therefore, one possible effect of ketocholestanol is an increase of about 4 \AA in the direction of the acyl chains of the hydrophilic width (polarity) of the interfacial region. With the hammock model described above, much of the helical region of the peptide must be located near the interfacial region of the bilayer. As noted by White and Wimley (5), the width of the polar headgroup region of PC bilayers is approximately the same as the diameter of the core of an α -helix. Thus, a 4 \AA increase in the width of the polar interfacial region has the effect of increasing the width of the potential energy barrier to the insertion of hydrophobic peptides into the bilayer. Given the configurational constraints outlined above for LamB-W, such an increase in interfacial width could mean that less of the hydrophobic amino acids in the α -helix would be exposed to the low-dielectric acyl chain region of the bilayer. This would decrease the contribution of the hydrophobic energy to the free energy of binding and tilt the energy balance in a manner such that the amount of peptide binding to the bilayer was markedly reduced. It follows that increasing the polarity of the acyl chain region near the hydrocarbon–water interface by the addition of hydrated dipoles, such as the ketone group in ketocholestanol, could cause a reduction in the hydrophobic free energy, which is the major factor

driving LamB-W binding to neutral bilayers (3). The addition of equimolar ketocholestanol reduced the free energy of transfer of LamB-W to EPC bilayers by about 2 kcal/mol (Table 1), a value that is comparable to the free energy of transfer (−1.9 kcal/mol) of a tryptophan residue from water to a PC bilayer (60). Therefore, if just a few nonpolar amino acid residues failed to become dehydrated as a result of an increase in the interfacial width, that could energetically account for the inhibitory effect of ketocholestanol.

The above arguments indicate that a key factor involved in ketocholestanol's effect on partitioning is not only the presence of its ketone dipole but also the dipole's location in the hydrocarbon region of the bilayer near the interface. The model described above is also consistent with two other observations. First, LamB-W binding was similar for SM/cholesterol bilayers and EPC and EPC/cholesterol bilayers (Figure 5A), even though the sphingosine backbone of SM has H-bonding characteristics and dipoles different from those of the glycerol backbone of EPC. This similarity most likely arises because the sphingosine backbone does not project any deeper into the bilayer than the deeper carbonyl groups in EPC, so the effective width of the polar headgroup region of the bilayer is similar for SM and EPC. The second, and more important observation, is that bilayers formed from 7-Doxyl PC (Figure 1) also did not appreciably bind LamB-W (Figure 5A). In this lipid, the dipolar nitroxide group would be expected to be located in the hydrocarbon region of the bilayer at about the same depth in the hydrocarbon region as the ketone in ketocholestanol (see the Results). Thus, bilayers formed from pure 7-Doxyl PC, like bilayers of EPC/ketocholestanol, should have a relatively wide interfacial region and thus reduce the free energy of transfer of the hydrophobic helix. Therefore, we argue that a key factor in binding of LamB to bilayers is the location of interfacial dipoles, which is not necessarily correlated with measured dipole potentials.

The properties of the interfacial region of bilayers could also be important in biological membranes, where several types of molecules with polar moieties could modify the effective width of the interfacial region. For example, transmembrane proteins or drugs that partition into the interfacial region could also introduce polar groups into the bilayer near the water–hydrocarbon interface.

Three Environments for Peptides Bound to Bilayers. In considering the partitioning of peptides into phospholipid bilayers, one must take into account three environments, each with distinct solvent properties: the aqueous phase, the acyl chain region, and the polar headgroup (interfacial region). The aqueous phase is a hydrogen-bonding solvent, the acyl chain region is apolar, whereas the interfacial region can have a wide variability in solvent properties because it contains charges, dipoles, hydrophobic groups (e.g., choline), H bond acceptors and donors, and a spatially varying dielectric constant that reflects a decreasing volume fraction of water closer to the acyl chain region. For peptides with some or part of their structure in the interfacial region (whose width is approximately the diameter of a peptide α -helix), the headgroup charges and dipoles can interact with those of the peptide and impart selectivity to peptide–bilayer interactions, as seen from the different behavior of the three LamB peptides in SDS and EPC and from the studies of Chaloin et al. (17). In this paper, we have shown that small changes

in composition near the interfacial region can disrupt the binding of LamB signal peptides to membranes. Thus, the width and hydration properties of the interfacial region can markedly effect the energetics of peptide–bilayer interactions.

ACKNOWLEDGMENT

We thank the Molecular Graphics Shared Resources facility of the Duke Cancer Center for molecular graphics of the LamB peptide and Dr. Vann Bennett for the use of CD equipment. We also thank Dr. Chris Nicchitta for helpful comments.

REFERENCES

- Jacobs, R. E., and White, S. H. (1989) *Biochemistry* 28, 3421–3437.
- De Kroon, A. I. P. M., Soekarjo, M. W., De Gier, J., and De Kruijff, B. (1990) *Biochemistry* 29, 8229–8240.
- Jones, J. D., and Gierasch, L. M. (1994) *Biophys. J.* 67, 1546–1561.
- Wang, Y., and Wiener, H. (1994) *Biochemistry* 33, 12860–12867.
- White, S. H., and Wimley, W. C. (1994) *Curr. Opin. Struct. Biol.* 4, 79–86.
- Dathe, M., Schumann, M., Wieprecht, T., Winkler, A., Beyermann, M., Krause, E., Matsuzaki, K., Murase, O., and Bienert, M. (1996) *Biochemistry* 35, 12612–12622.
- Ben-Shaul, A., Ben-Tal, N., and Honig, B. (1996) *Biophys. J.* 71, 130–137.
- Kim, P. K., Janiak-Spens, F., Trimble, W. S., Leber, B., and Andrews, D. W. (1997) *Biochemistry* 36, 8873–8882.
- Ben-Tal, N., Honig, B., Miller, C., and McLaughlin, S. (1997) *Biophys. J.* 73, 1717–1727.
- Heymann, J. B., Zakharov, S. D., Zhang, Y.-L., and Cramer, W. A. (1996) *Biochemistry* 35, 2717–2725.
- Kim, J., Mosior, M., Chung, L. A., Wu, H., and McLaughlin, S. (1991) *Biophys. J.* 60, 135–148.
- Ben-Tal, N., Honig, B., Peitzsch, R. M., Denisov, G., and McLaughlin, S. (1996) *Biophys. J.* 71, 561–575.
- Demel, R. A., Goormaghtigh, E., and de Kruijff, B. (1990) *Biochim. Biophys. Acta* 1027, 155–162.
- Killian, J. A., Keller, R. C. A., Struyve, M., deKroon, A. I. P. M., Tommassen, J., and deKruijff, B. (1990) *Biochemistry* 29, 8131–8137.
- Keller, R. C. A., ten Berge, D., Nouwen, N., Snel, M. M. E., Tommassen, J., Marsh, D., and de Kruijff, B. (1996) *Biochemistry* 35, 3063–3071.
- Evans, E., Rawicz, W., and Hofmann, A. F. (1995) Lipid bilayer expansion and mechanical disruption in solutions of water-soluble bile acid, in *Bile Acids in Gastroenterology* (Hofmann, A. F., Paumgartner, G., and Stiehl, A., Eds.) pp 59–68, Cluver Academic, Boston.
- Chaloin, L., Vidal, P., Heitz, A., Van Mau, N., Mery, J., Divita, G., and Heitz, F. (1997) *Biochemistry* 36, 11179–11187.
- von Heinje, G. (1985) *J. Mol. Biol.* 184, 99–105.
- Wickner, W., and Leonard, M. R. (1996) *J. Biol. Chem.* 271, 29514–29516.
- Schatz, P., and Beckwith, J. (1990) *Annu. Rev. Genet.* 24, 215–248.
- Joly, J. C., and Wickner, W. (1993) *EMBO J.* 12, 255–263.
- Hanein, D. (1996) *Cell* 87, 721–732.
- Martoglio, B., Hofmann, M. W., Brunner, J., and Dobberstein, B. (1995) *Cell* 81, 207–214.
- McKnight, C. J., Stradley, S. J., Jones, J. F., and Gierasch, L. M. (1991) *Proc. Natl. Acad. Sci. U.S.A.* 88, 5799–5803.
- Jones, J. D., and Gierasch, L. M. (1994) *Biophys. J.* 67, 1534–1545.
- Briggs, M. S., Gierasch, L. M., Zlotnick, A., Lear, J. D., and DeGrado, W. F. (1985) *Science* 228, 1096–1099.
- McKnight, C. J., Briggs, M. S., and Gierasch, L. M. (1989) *J. Biol. Chem.* 264, 17293–17297.

28. McKnight, C. J., Rafalski, M., and Gierasch, L. M. (1991) *Biochemistry* 30, 6241–6246.
29. Wang, Z., Jones, J. D., Rizo, J., and Gierasch, L. M. (1993) *Biochemistry* 32, 13991–13999.
30. Hristova, K., Selsted, M. E., and White, S. H. (1996) *Biochemistry* 35, 11888–11894.
31. New, R. R. C. (1990) *Liposomes: a Practical Approach*, IRL Press, New York.
32. Chen, P. S., Toribara, T. Y., and Warner, H. (1956) *Anal. Chem.* 28, 1756–1758.
33. Hope, M. J., Bally, M. B., Webb, G., and Cullis, P. R. (1985) *Biochim. Biophys. Acta* 812, 55–65.
34. McIntosh, T. J., and Simon, S. A. (1986) *Biochemistry* 25, 4058–4066.
35. McIntosh, T. J., Simon, S. A., Needham, D., and Huang, C.-h. (1992) *Biochemistry* 31, 2012–2020.
36. Simon, S. A., McIntosh, T. J., Magid, A. D., and Needham, D. (1992) *Biophys. J.* 61, 786–799.
37. McIntosh, T. J. (1980) *Biophys. J.* 29, 237–246.
38. Sophianopoulos, J. A., Durham, S. J., Sophianopoulos, A. J., Ragsdale, H. L., and Cropper, W. P. (1978) *Arch. Biochem. Biophys.* 187, 132–137.
39. Ladokhin, A. S., Selsted, M. E., and White, S. H. (1997) *Biophys. J.* 72, 794–805.
40. White, S. H., Wimley, W. C., Lasokhin, A. S., and Histrova, K. (1998) *Methods Enzymol.* 295, 62–88.
41. Hunter, R. J. (1991) *Foundations of Colloid Science*, Oxford Press, New York.
42. Eisenberg, M., Gresalfi, T., Riccio, T., and McLaughlin, S. (1979) *Biochemistry* 18, 5213–5223.
43. MacDonald, R. C., and Simon, S. A. (1987) *Proc. Natl. Acad. Sci. U.S.A.* 84, 4089–4094.
44. Chang, C. T., Wu, C.-S. C., and Yang, J. T. (1978) *Anal. Biochem.* 91, 13–31.
45. Lakowicz, J. R. (1983) *Principles of Fluorescence Spectroscopy*, Plenum Press, New York.
46. Vogel, H. (1981) *FEBS Lett.* 134, 37.
47. Tatulian, S. A. (1987) *Biochim. Biophys. Acta* 901, 161–165.
48. Israelachvili, J. N. (1991) *Intermolecular and Surface Forces*, Academic Press, London.
49. Evans, E. (1991) *Langmuir* 7, 1900–1908.
50. Needham, D. (1995) Cohesion and permeability of lipid bilayer vesicles, in *Permeability and stability of lipid bilayers* (Disalvo, E. A., and Simon, S. A., Eds.) pp 49–76, CRC Press, Boca Raton, FL.
51. McIntosh, T. J., Advani, S., Burton, R. E., Zhelev, D. V., Needham, D., and Simon, S. A. (1995) *Biochemistry* 34, 8520–8532.
52. Lentz, B. R., McIntyre, G. F., Parks, D. J., Yates, J. C., and Massenburg, D. (1992) *Biochemistry* 31, 2643–2653.
53. Franklin, J. C., and Cafiso, D. S. (1993) *Biophys. J.* 65, 289–299.
54. Franks, N. P. (1976) *J. Mol. Biol.* 100, 345–358.
55. Worcester, D. L., and Franks, N. P. (1976) *J. Mol. Biol.* 100, 359–378.
56. Cafiso, D. S. (1995) Influence of charges and dipoles on macromolecular adsorption and permeability, in *Permeability and stability of lipid bilayers* (Disalvo, E. A., and Simon, S. A., Eds.) pp 179–196, CRC Press, Boca Raton, FL.
57. Lewis, B. A., and Engelman, D. M. (1983) *J. Mol. Biol.* 166, 211–217.
58. Tardieu, A., Luzzati, V., and Reman, F. C. (1973) *J. Mol. Biol.* 75, 711–733.
59. Shoemaker, K. R., Kim, P. S., York, E. J., and Baldwin, R. L. (1987) *Nature* 326, 563–567.
60. Wimley, W. C., Creamer, T. P., and White, S. H. (1996) *Biochemistry* 35, 5109–5124.
61. Smejtek, P. (1995) Permeability of lipophilic ions across lipid bilayers, in *Permeability and stability of lipid bilayers* (Disalvo, E. A., and Simon, S. A., Eds.) pp 197–240, CRC Press, Boca Raton, FL.
62. Engelman, D. M., and Steitz, T. A. (1981) *Cell* 23, 411–422.
63. Hunt, J. F., Rath, P., Rothschild, K. J., and Engleman, D. M. (1997) *Biochemistry* 36, 15177–15192.
64. Wimley, W. C., and White, S. H. (1993) *Biochemistry* 32, 6307–6312.
65. MacNaughtan, W., Snook, K. A., Caspi, E., and Franks, N. P. (1985) *Biochim. Biophys. Acta* 818, 132–148.
66. Newton, A. C. (1995) *J. Biol. Chem.* 270, 28495–28498.
67. McLaughlin, S., and Aderem, A. (1995) *Trends Biochem. Sci.* 20, 272–276.
68. MacDonald, R. C., Simon, S. A., and Baer, E. (1976) *Biochemistry* 15, 855–869.
69. Cladera, J., and O'Shea, P. (1998) *Biophys. J.* 74, 2434–2442.
70. Flewelling, R. F., and Hubbell, W. L. (1986) *Biophys. J.* 49, 541–552.
71. Antosiewicz, J., and Porshke, D. (1989) *Biochemistry* 28, 10072–10078.
72. Needham, D., and Nunn, R. S. (1990) *Biophys. J.* 58, 997–1009.
73. McIntosh, T. J., Simon, S. A., Needham, D., and Huang, C.-h. (1992) *Biochemistry* 31, 2020–2024.
74. Simon, S. A., and McIntosh, T. J. (1989) *Proc. Natl. Acad. Sci. U.S.A.* 86, 9263–9267.

BI9805792